

Myofibrillogenesis Regulator-1 in Smooth Muscle Cells Modulates Inflammation Signaling Pathways via Regulating ROCK1 Ubiquitination and Degradation to Impact Aortic Dissection

Hang Yin^{1-5,*}, Xiaoxing Li^{6,*}, Dazhou Lu^{1-5,*}, Xin Zhao^{7,*}, Zeyu Yang¹⁻⁵, Zerui Wang¹⁻⁵, Feng Xu¹⁻⁵, Yuguo Chen¹⁻⁵, Chuanbao Li¹⁻⁵

¹Department of Emergency Medicine, Qilu Hospital of Shandong University, Jinan, People's Republic of China; ²Shandong Provincial Clinical Research Center for Emergency and Critical Care Medicine, Institute of Emergency and Critical Care Medicine of Shandong University, Chest Pain Center, Qilu Hospital of Shandong University, Jinan, People's Republic of China; ³Key Laboratory of Emergency and Critical Care Medicine of Shandong Province, Key Laboratory of Cardiopulmonary-Cerebral Resuscitation Research of Shandong Province, Shandong Provincial Engineering Laboratory for Emergency and Critical Care Medicine, Qilu Hospital of Shandong University, Jinan, People's Republic of China; ⁴Shandong Key Laboratory: Magnetic Field-Free Medicine & Functional Imaging (MF), Qilu Hospital of Shandong University, Jinan, People's Republic of China; ⁵NMPA Key Laboratory for Clinical Research and Evaluation of Innovative Drug, Qilu Hospital of Shandong University, Jinan, People's Republic of China; ⁶Department of Geriatrics, Qilu Hospital, Shandong University, Jinan, Shandong, People's Republic of China; ⁷Department of Cardiovascular Surgery, Qilu Hospital of Shandong University, Jinan 250012, Shandong, People's Republic of China

*These authors contributed equally to this work

Correspondence: Chuanbao Li; Yuguo Chen, Department of Emergency Medicine, Qilu Hospital of Shandong University, Jinan, People's Republic of China, Email bao2460@126.com; chen919085@sdu.edu.cn

Background: Aortic dissection (AD) is a life-threatening cardiovascular emergency and currently lacks effective drug treatment. Inflammation is a critical mechanism in the development of AD, and identifying specific molecular targets to regulate inflammation is crucial for stopping its progression. This study aimed to investigate the role of MR-1 and ROCK1 in the regulation of inflammation in AD and their potentialities as therapeutic targets.

Methods: Researchers performed protein immunoblotting on aortic wall tissue from 10 patients who underwent aortic arch replacement and 10 patients who underwent coronary artery bypass grafting to examine the expression levels of MR-1, ROCK1, and inflammatory pathways in the aortas. In vitro experiments, human aortic smooth muscle cells were extracted, and an in vitro dissection model was constructed with angiotensin II. siRNA silencing studies were performed to investigate the effects of MR-1 and ROCK1 on the development of AD and their interconnections.

Results: Analysis of aortic tissues revealed significantly elevated levels of MR-1 and ROCK1 in AD patients, and meanwhile the inflammatory indexes showed the same trend. Furthermore, it was observed that overexpression of MR-1 and ROCK1 facilitated smooth muscle cell phenotypic transformation and augmented matrix metalloproteinase release in in vitro settings through inflammatory pathway activation. The relationship between MR-1 and ROCK1 was elucidated, too.

Conclusion: MR-1 and ROCK1 overexpression is associated with the occurrence and development of AD through inflammation. This study highlights the role of inflammation in AD development and tap the potentiality of using MR-1 and ROCK1 as targets to alleviate AD development.

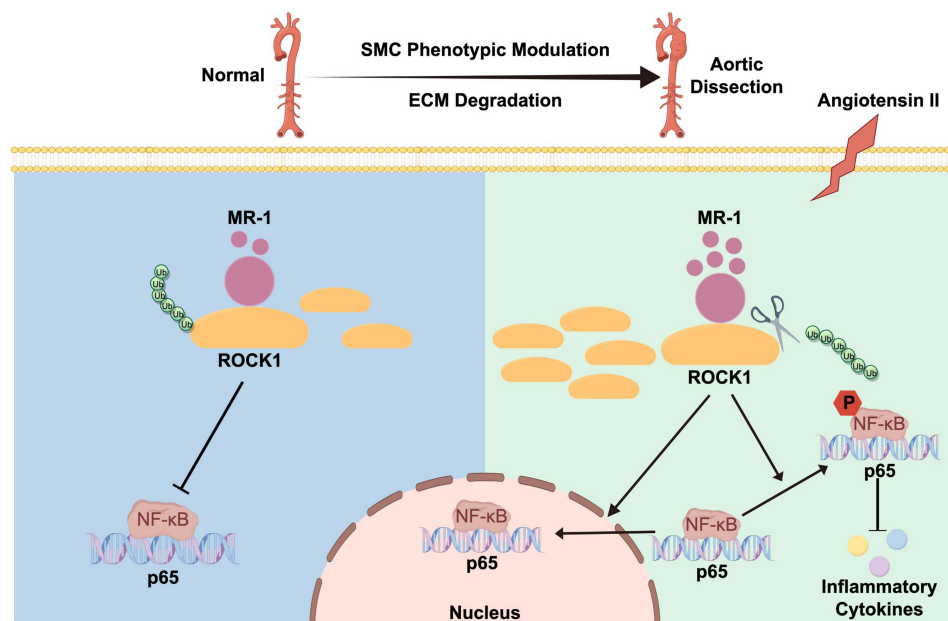
Keywords: MR-1, ROCK1, aortic dissection, inflammation, phenotypic switch

Introduction

Aortic dissection remains a critical and often fatal cardiovascular emergency, with an annual incidence of 3 in 100,000.¹ The potential rupture of the aortic adventitia leading to bleeding at any moment contributes to the high mortality rate associated with AD. Untreated acute dissection can result in a mortality rate exceeding 20% within 6 hours. Surgical



Graphical Abstract



intervention is currently the primary mode of treatment for AD. The aortic wall is a dynamic structure that comprises a complex network of cells and extracellular matrix, each serving specific biomechanical functions to ensure appropriate compliance and strength in response to hemodynamic changes.² Comprising three layers—the thin intima, the myoelastic media, and the fibrous outer layer—the aortic wall is a sophisticated system.³ The intima, characterized by abundant smooth muscle cells and extracellular matrix, plays a crucial role in maintaining the normal function and structure of the aortic vessel wall.⁴ In the pathological condition of aortic dissection, the middle layer of the entrapped artery exhibits inflammatory characteristics, including the apoptosis of vascular smooth muscle cells (vSMCs), leukocyte infiltration, and heightened expression of matrix metalloproteinases (MMPs).^{5–7} The inflammatory response within the aortic wall has emerged as a prominent research focus in recent years, shedding light on the pathogenesis of aortic dissection. Anti-inflammatory therapy has garnered attention as a potential strategy for the treatment of aortic dissection. For instance, studies have indicated that the application of dexamethasone has the potentiality to reduce aortic dissection formation in mice.⁸ The incorporation of emerging research trends and potential treatment strategies has the potentiality to advance our understanding and management of aortic dissection, ultimately improving patient outcomes.

Myofibrillogenesis regulator-1 (MR-1), a protein comprising 142 amino acids, has been identified from a human skeletal muscle cDNA library. Intracellularly, MR-1 is primarily distributed in the nuclear membrane and the cytoplasm. Northern blot and sequence analysis of gene expression have indicated that the transcript levels of MR-1 are particularly high in cardiac muscle and skeletal muscle. However, the expression and role of MR-1 in smooth muscle cells have not been fully explored.⁹ In vitro yeast two-hybrid screening and in vitro GST pull-down assays have revealed that MR-1 primarily functions by regulating myosin light chain. The expression of myosin light chain has been identified as a key factor that influences the role of smooth muscle cells. Previous research has also suggested that MR-1 plays a role in cardiovascular disease progression through its regulation of inflammatory pathways.^{10,11} Based on these findings, it can be inferred that MR-1 may be expressed to some extent in smooth muscle cells and could potentially regulate their function. However, a comprehensive understanding of this regulatory mechanism is yet to be established. Further studies are required to elucidate the role of MR-1 in smooth muscle cells and its potential impact on cardiovascular disease progression. These potential interactions could offer new insights into cardiovascular pathology and potential avenues for

therapeutic intervention. Such investigation will provide a comprehensive perspective on the significance of MR-1 in the context of smooth muscle cells and its interplay within the broader cardiovascular system.

As a critical downstream effector of RhoA within the small G protein family, Rho-associated protein kinase (ROCK) is known to be abnormally activated in numerous cardiovascular conditions, including atherosclerosis, hypertension, cardiac hypertrophy, and arrhythmogenic right ventricular cardiomyopathy.¹² Both ROCK 1 and ROCK 2 isoforms are significantly expressed in vascular smooth muscle and myocardium.¹³ Studies have revealed that ROCK 1 plays a pivotal role in regulating smooth muscle cell functions by influencing inflammation, myosin phosphorylation, cell proliferation, migration, and phenotypic transformation of smooth muscle cells.^{14–16} Given the significant role of inflammatory pathways in aortic dissection AD, it is reasonable to suspect that ROCK 1 may influence the development and progression of AD through its regulation of smooth muscle cell function. However, the specific mechanisms through which ROCK 1 impacts the development of AD require further elucidation. Understanding the precise interplay between ROCK 1 and smooth muscle cells in the context of AD could provide valuable insights into the pathogenesis of this life-threatening condition and potentially pave the way for new therapeutic interventions. Exploring these interactions will significantly contribute to our comprehension of the role of ROCK 1 in AD and cardiovascular diseases and might offer potential avenues for targeted treatments. Further investigation into the involvement of ROCK 1 in the context of smooth muscle cells and its potential impact on the pathogenesis of AD will serve to bolster our overall understanding of these complex interplays within the cardiovascular system.

Materials and Methods

Human Aortic Collection

In accordance with the Declaration of Helsinki, human aortic tissue was obtained with informed consent according to a protocol approved by the Ethics Committee of Qilu Hospital, Shandong University (Catalog: KYLL-202208-005). A total of 27 patients were screened during the period from September 2022 to September 2023. Three patients were excluded from further analysis because their aortic disease was aortic aneurysm, and 4 patients were withdrawn because they refused to sign the informed consent form. A total of 20 patients were ultimately included in this analysis, including 10 AD patients and 10 non-AD controls (NC). Aortic dissection tissue was obtained from 10 AD patients who underwent Wheat or Bentall surgery for aortic dissection confirmed by coronary CTA. Non-clamped aortic samples were obtained from 10 patients with coronary atherosclerotic heart disease or heart valve disease who underwent CABG at our institution. All samples were aseptically resected intraoperatively, were aortic wall tissue, rinsed with cold sterile phosphate-buffered saline (PBS) (G4202-500ML, Servicebio, Wuhan, China) to remove blood components, and immediately preserved in liquid nitrogen or 4% paraformaldehyde (PFA) (BL539A, Biosharp, Hefei, China). The baseline demographic characteristics of the AD group and the control group are shown in [Table 1](#).

Cell Isolation and Culture

Human aortic tissue was carefully dissected and placed in a 50mL centrifuge tube containing PBS. The tissue was manipulated within an ultra-clean bench to maintain sterility. The aortic tissue was then transferred to a 10 mm cell culture dish and washed three times with sterile PBS containing 1% penicillin/streptomycin. The aortic intima was gently removed using curved forceps, while the aortic media was preserved. The media was then transferred to high glucose Dulbecco's modified Eagles medium (DMEM) (Gibco, containing 2mM L-glutamine, 4.5 g/L D-glucose and 110 mg/L sodium pyruvate) supplemented with 10% fetal bovine serum (FBS) (Gibco, Australia) and cut into small pieces using ophthalmic scissors. The tissue was washed with PBS and subjected to digestion with 0.15% collagenase II (V900892-1G, Sigma Aldrich, USA) at 37°C for 10 hours. Following digestion, the tissue mass was dissociated by repeated pipetting and centrifuged. The resulting cells were resuspended in smooth muscle cell medium (1101, ScienCell, USA) and cultured in T25 cell culture flasks under standard conditions (37°C, 5% CO₂, saturated humidity).

Table 1 Baseline Characteristics

Variables	AD (N=10)	NC (N=10)	P value
Age, years	58.70±11.86	61.40±10.72	0.950
Male gender, n(%)	8 (80.00%)	6 (60.00%)	0.628
BMI (kg/m ²)	26.41±4.96	24.26±2.39	0.016*
Smoking, n(%)	9 (90.00%)	6 (60.00%)	0.303
CAD, n(%)	0 (0.00%)	10 (100.00%)	0.000*
HP, n(%)	1 (10.00%)	3 (30.00%)	0.582
DM, n(%)	3 (30.00%)	7 (70.00%)	0.179
HL, n(%)	6 (60.00%)	7 (70.00%)	1
WBC (*10 ⁹ /L)	11.33±3.99	9.05±2.34	0.038*
NEU (*10 ⁹ /L)	9.67±1.17	6.19±2.41	0.049*
MONO (*10 ⁹ /L)	0.66±0.08	0.67±0.12	0.187
LYM (*10 ⁹ /L)	0.95±0.12	2.02±0.24	0.039*

Notes: Data are expressed as mean ± standard deviation or absolute numbers (proportions). *P < 0.05.

Abbreviations: AD, aortic dissection disease; NC, negative control; BMI, body mass index; CAD, coronary atherosclerotic heart disease; HP, hypertension; DM, diabetes mellitus; HL, hyperlipidemia; WBC, leukocytes; NEU, neutrophils; MONO, monocytes; LYM, lymphocytes.

RNA Isolation and Quantitative Real-Time Reverse Transcription PCR

Human aortic smooth muscle cells (HASMCs) were cultured and harvested for RNA isolation using the Trizol Reagent (Invitrogen, USA) following a standard protocol. Total RNA was extracted and quantified using spectrophotometric analysis, and its integrity was assessed using gel electrophoresis. The RNA was then subjected to reverse transcription using stem-loop primers and the subsequent PCR analysis. Reverse transcription and PCR were carried out using HiScript II Q RT SuperMix for qPCR and ChamQ Universal SYBR qPCR Master Mix (Vazyme, NA).

Western Blotting

Aortic tissues and HASMCs were rinsed with cold 1×PBS, and then lysed on ice in radioimmunoprecipitation assay (RIPA) lysis buffer (Beyotime Biotech) comprising 50mM Tris (pH 7.4), 150mM NaCl, 1% Triton X-100, 1% sodium deoxycholate, 0.1% sodium dodecyl sulfate (SDS), 1mM sodium orthovanadate, 1mM sodium fluoride, 1mM Ethylenediaminetetraacetic acid (EDTA), and leupeptin, along with 1mM phenylmethylsulfonyl fluoride (PMSF) for 15 minutes. The samples were then homogenized with 20 kHz ultrasonic lapping and centrifuged at 14,000 rpm at 4°C in a refrigerated microcentrifuge for 15 minutes to extract total protein. Supernatants were stored, and the protein concentration was determined using the bicinchoninic acid (BCA) Protein Assay Kit (Beyotime Biotech) to normalize the samples. Equal amounts of protein were added to 4x loading buffer (PR20003, Proteintech, Wuhan, China), boiled for 10 minutes, and separated by SDS-PAGE at 90V for 30 minutes, followed by 120V for 1 hour, then transferred to polyvinylidene difluoride (PVDF) membranes using a wet-transfer system. The membranes were blocked for 30 minutes with QuickBlock Blocking Buffer (Beyotime Biotech) at room temperature. Primary antibodies were diluted proportionally and incubated with the membranes at 4°C overnight. After washing with Tris-buffered saline-Tween-20 (TBST) (Servicebio, Wuhan, China), the membranes were incubated with the corresponding secondary antibodies coupled with horseradish peroxidase (HRP) for 90 minutes on shakers. Following another wash with TBST, enhanced chemiluminescence (ECL) signals were detected using an ECL kit (Millipore, Billerica, MA, USA) and an Imaging system (Thermo Fisher Scientific). Densitometric quantification was performed using Image J software.

Co-Immunoprecipitation (Co-IP)

Human vSMCs were collected after culturing in T25 culture flasks, and then fully lysed by incubation with NP-40 lysis solution (Beyotime, Shanghai, China) for 1 h at 4°C on the rotating mixer. The supernatant was separated by centrifugation at 14,000 rpm for 15 min at 4°C, and the appropriate amount of primary antibody was added and incubated overnight at 4°C. Subsequently, PureProteome Protein A/G MixMagnetic Beads (Merck Millipore, USA) were added to the supernatant and incubated at 4°C for 3 h to make the proteins bind to the magnetic beads. Following this, the magnetic beads were separated by the magnetic rack, and then the samples were separated from the magnetic beads by adding PBS-diluted SDS-PAGE loading buffer (4x)(Proteintech, Wuhan, China) to the beads and incubating at 100°C for 10 min. Ultimately, the protein samples were subjected to SDS-PAGE, and the subsequent steps were identical to those employed in Western blotting. The data was analysed using Image J software.

Histological Staining of Collagen and Elastin

Aortic samples were initially fixed in 4% paraformaldehyde and then underwent a series of processing steps including dehydration, paraffin embedding, and subsequent sectioning at a thickness of 5 µm. The study employed Hematoxylin and Eosin (HE) staining (DH0006, Leagene Biotechnology, Beijing, China) to assess the aortic structure and morphology. Additionally, Masson's trichrome staining kit (DC0032-100, Leagene, Beijing, China) was employed to measure collagen deposition as per the manufacturer's instructions. Finally, all sections were observed under a slice scanner (VS200, Olympus, Japan).

Immunohistochemistry

Human aortic tissue sections were subjected to a series of treatments to facilitate immunohistochemical staining. The paraffin sections were first removed and baked in an oven at 65°C for 30 minutes to prevent deparaffinization. The slices were then placed in a dewaxing solution and baked overnight in an oven at 65°C, followed by gradient alcohol hydration. Subsequent to several washes in PBS, membrane-breaking treatment was conducted using 0.1% TritonX-100 at room temperature for 10 minutes. To block non-specific binding sites, paraffin sections were treated with 5% bovine serum albumin (BSA) (AR0197, Boster Biological Technology, Wuhan, China) for 30 minutes. After blocking, primary antibodies against MR-1 and ROCK1, diluted at optimized concentrations in 1% BSA, were incubated with the sections in a wet box overnight at 4°C. Following this, the appropriate secondary antibody was applied and incubated at room temperature for 30 minutes. The positive staining was detected using a DAB Kit (AR1027-3, Boster Biological Technology, Wuhan, China), and nuclear counterstaining was performed using hematoxylin staining. Lastly, counterblue solution (G1040-500ML, Service bio, Wuhan, China) was applied for 5 minutes at room temperature. The immunohistochemically stained images were visualized and captured using an Olympus microscope, and the obtained data were quantified using Image J software.

Immunofluorescence

Human aortic tissues and HASMCs were subjected to a series of treatments to facilitate immunofluorescence staining. The cells and tissues were initially rinsed with 1×PBS, followed by fixation using 4% PFA at room temperature for 15 minutes. Subsequently, membrane permeabilization was achieved using 0.25% TritonX-100 at room temperature for 30 minutes. To block non-specific binding sites, a 10% goat serum solution was applied at room temperature for 30 minutes. After blocking, primary antibodies against IL-1β (ab254360, Abcam, UK), IL-6 (ab233706, Abcam, UK), and TNF-α (ab183218, Abcam, UK) were diluted at optimized concentrations in 1% BSA and incubated with the samples overnight at 4°C. Following this, fluorescent marker-labeled goat anti-rabbit secondary antibody was applied and incubated at room temperature for 45 minutes. DAPI (ab104139, Abcam, UK) was used as the nuclear counterstain to visualize the nuclei, and an anti-fading mounting medium was used to seal the samples. Finally, the immunofluorescently stained samples were imaged using a fluorescence confocal microscope (STELLARIS 8, Leica Microsystems CMS GmbH, Germany).

Statistical Analysis

Clinical data were statistically analyzed using SPSS software version 26. (For demographic and clinical characteristics, continuous variables were expressed as mean±SD or median with its interquartile range (IQR) if the normal distribution was not met, and categorical variables were expressed as numbers and percentages. Independent samples *t*-test was used for comparison between the two groups). Data obtained from the experimental phase were subjected to statistical analysis using GraphPad Prism 9.0 software (GraphPad Inc., La Jolla, CA, USA). Continuous variables were expressed as mean ± SEM, while categorical variables were expressed as absolute numbers and percentages. All data are based on biological replicates. The data were initially tested for normality utilizing the Shapiro–Wilk test, and variance alignment was assessed using the F-test. The Student's *t*-test was used to define differences between 2 datasets. For 3 or more datasets, one-way ANOVA followed by Bonferroni post hoc test for multiple comparisons was used. $p < 0.05$ was considered statistically different (* $P < 0.05$, ** $P < 0.01$, *** $P < 0.001$, **** $P < 0.0001$).

Results

Baseline Characteristics of Study Population

The baseline clinical characteristics of the study population are outlined in [Table 1](#), highlighting the demographics and key health metrics of the 20 patients included in the study. This cohort comprised 10 patients diagnosed with aortic dissection and 10 non-AD controls, covering an age range from 38 to 76 years. On average, the AD patients had a mean age of 58.70 ± 11.86 , while the NC patients averaged 61.40 ± 10.72 ($P = 0.950$). Encouragingly, both patient groups had a predominantly male composition (80.00% in the AD group and 60.00% in the NC group, $P = 0.628$), consistent with the gender distribution often observed in cardiovascular health studies. Furthermore, the majority of patients across both groups were smokers, with rates at 90.00% and 60.00% in the AD and NC groups, respectively ($P = 0.303$). Additionally, a considerable portion of both cohorts were identified as hyperlipidemic, with values at 60.00% and 70.00%, respectively ($P = 1$). These shared attributes present an initial key insight into the commonalities observed in cardiovascular risk profiles among AD and NC patients. Interestingly, the statistical analysis revealed several important differences between the two groups. Specifically, while differences in monocyte count were not significant, the study unveiled statistically significant variations in key inflammation indicators, such as leukocyte levels (11.33 ± 3.99 in AD patients, 9.05 ± 2.34 in NC patients, $P = 0.038$), neutrophil counts ($P = 0.049$), and lymphocyte counts ($P = 0.039$). Moreover, BMI levels also showed significant divergence, with AD patients presenting a mean BMI of 26.41 ± 4.96 compared to 24.26 ± 2.39 in the NC group ($P = 0.016$). Notably, the presence of coronary artery disease demonstrated a significant difference, showcasing 0% occurrence in the AD group compared to 100% in the NC group ($P = 0.000$). These striking statistical results indicate the pivotal role of inflammation as a contributory mechanism in the pathogenesis of aortic dissection. The results underscore the importance of considering cardiovascular risk factors and inflammation as critical facets of the disease process and pave the way for further exploration of these avenues in next research.

Differences in Aortic Tissue Structural Changes and Inflammatory Infiltration Between AD and Non-AD Humans

Initially, structural staining was performed on aortic tissue from AD and Ctrl patients. HE staining demonstrated a torn aortic wall layer in AD tissue, typified by a disorderly cell arrangement, substantial destruction of the extracellular matrix, and a significantly reduced number of smooth muscle cells. In stark comparison, the Ctrl group displayed a tightly organized membrane arrangement with a higher number of smooth muscle cells. Additionally, MASSON staining revealed a deep blue staining of the aortic wall in the AD group, indicating a large percentage of area and significant collagen fiber hyperplasia. Conversely, the Ctrl group exhibited lighter blue staining, a smaller percentage of area, an increased amount of red staining, and a larger proportion of muscle fibers in comparison to the dissection group ([Figure 1A](#)). Subsequently, immunofluorescence staining of inflammatory cytokines was carried out on aortic tissues extracted from both groups, revealing markedly elevated levels of NF-kappaB p65 activation and increased expression of inflammatory factors TNF- α , IL-1 β , and IL-6 in the aortic tissues of the AD group as opposed to the Ctrl group ([Figure 1B](#) and [C](#)). Moreover, protein immunoblotting was employed to assess the protein expression level of tissue

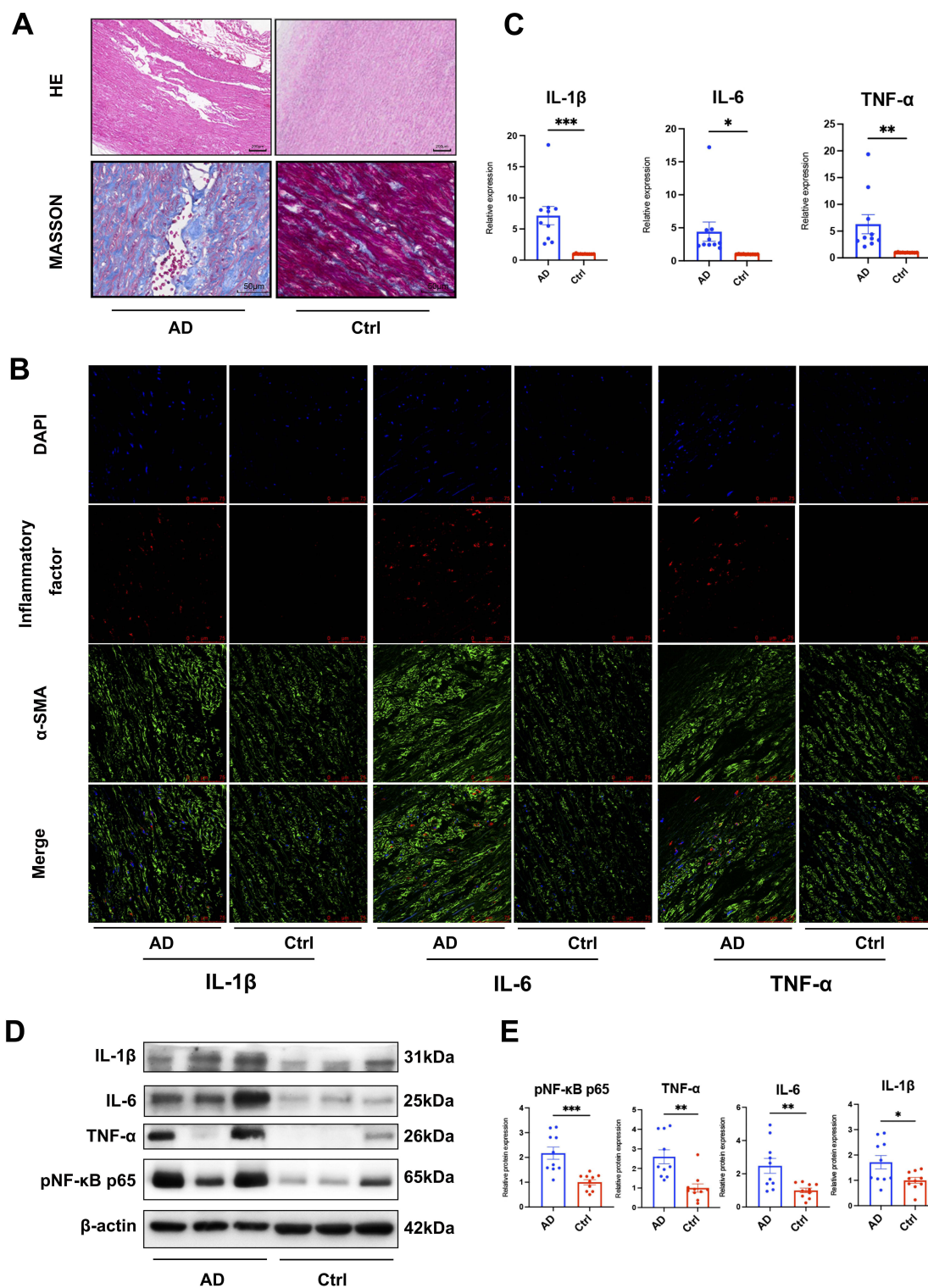


Figure 1 Differences in structural and inflammatory expression levels in the aorta between AD and non-AD groups. **(A)** HE staining and MASSON staining of human aorta in AD and Ctrl groups. **(B)** Immunofluorescence staining and **(C)** quantification of IL-1 β (red), IL-6 (red) and TNF- α (red) in human aortas in AD or Ctrl groups (unpaired two-tailed Student's *t*-test with Welch's correction for IL-1 β , IL-6 and TNF- α). Scale bar = 75 μ m. Each datapoint represents an individual human. n=10 human aortas (AD or Ctrl). **(D)** Western blot analysis and **(E)** quantification of pNF- κ B p65, IL-1 β , IL-6, and TNF- α in human aortas with AD or Ctrl (unpaired two-tailed Student's *t*-test with Welch's correction for pNF- κ B p65, IL-1 β , IL-6 and TNF- α). β -actin was used as a loading control. Data are shown as mean \pm SEM. Each datapoint represents an individual human. n=10 human aortas (AD or Ctrl). All data are based on biological replicates. The duplication occurred in **Figures 1D and 2C E** (β -actin) because the experimental conditions and sample sources for these groups were consistent. **P* < 0.05, ***P* < 0.01, ****P* < 0.001.

inflammatory factors in all 20 patients (Figure 1D and E). The obtained results concurred with those from immunostaining, corroborating the increased presence of these inflammatory factors in the AD group (Figure 1D and E). These findings collectively underscore the pivotal role of inflammation in the development of AD and, more specifically, its potential contribution to structural alterations observed in aortic tissues. This suggests a critical connection between inflammation and cardiovascular health, presenting a compelling argument for further exploration of these mechanisms as crucial factors in the pathogenesis of AD.

MR-1 and ROCK1 are Elevated in Human Intercalated Aortas

To explore the potential involvement of MR-1 and ROCK1 in human aortic dissection, our study embarked by examining the protein expression of MR-1 and ROCK1 in both AD and Ctrl human aortic tissues. Notably, our immunohistochemical examinations revealed a marked increase in the expression levels of both MR-1 and ROCK1 in the region of aortic dissection in AD as compared to Ctrl aorta (Figure 2A and B). Consistently, protein immunoblotting analysis conducted on aortic samples procured from 20 patients demonstrated a noticeable elevation in the expression of both MR-1 and ROCK1 within the AD group (See Figure 2C and D). These findings collectively indicate that the expression of MR-1 and ROCK1 is significantly heightened in the context of aortic dissection, thereby implicating a potential contribution of these proteins to the progression of the condition. This elevated expression underscores their putative roles in the pathogenesis of AD and may provide critical insights into the underlying molecular mechanisms driving its development.

Smooth Muscle Cell Extraction and Protein Expression in the Context of an Aortic Dissection Model

Human smooth muscle cells were extracted from human aortic tissue and subjected to immunofluorescence staining to detect α -SMA, a known marker for vSMCs. The results revealed that nearly 100% of the isolated cells expressed α -SMA, confirming their identity as vSMCs (See Figure 2E). This validation underscores the suitability of these cells for further cytological investigations. We stimulated human aortic smooth muscle cells with 1 μ mol/L angiotensin for 24 hours to establish a model mimicking the complex pathophysiology of AD. This model sought to replicate the conditions present in human aortic smooth muscle cells in the development and progression of AD. We utilized Western Blotting to quantitatively measure the expression levels of MR-1 and ROCK1, and to assess the activation levels of inflammatory pathways in AD vSMCs in vitro model. The investigative results highlighted a significant elevation in the expression levels of MR-1 and ROCK1, along with heightened activation of inflammatory pathways within the AD group, as compared to the Ctrl group (See Figure 2F and G). This outcome is in accordance with data obtained from comprehensive organizational testing.

MR-1 Affects Smooth Muscle Cell Phenotypic Transformation and Matrix Metalloproteinase Release by Regulating Inflammatory Factor Release

In order to delineate the specific mechanisms by which MR-1 influences the formation of AD, we undertook a series of experiments. Based on AD cell model, we conducted protein immunoblotting to gauge MR-1 expression levels across various treated groups. Our analysis encompassed the examination of MR-1 protein expression in normal human aortic smooth muscle cells (control group), dissected human aortic smooth muscle cells (AD group), intercalated human aortic smooth muscle cells treated with MR-1 siRNA 1/2 (MR-1 siRNA 1/2 group), and MR-1 siRNA Negative Control (MR-1 NC group). Notably, we observed a substantial increase in MR-1 expression in the AD and MR-1 NC groups as compared to the control and MR-1 siRNA 1/2 groups. Concurrently, we found altered expression patterns of smooth muscle cell phenotypic transformation markers, including α -SMA, OPN, and matrix metalloproteinase 9 (MMP9), which correlated with MR-1 expression levels. Specifically, compared with the AD group, the expression of α -SMA was upregulated in the MR-1 siRNA 1/2 group, while the expressions of OPN and MMP9 were downregulated (See Figure 3A and B). These findings underscore the potential role of MR-1 in modulating AD formation through its influence on smooth muscle cell phenotypic transformation and extracellular matrix degradation. Furthermore, we sought to investigate the potential pathways through which MR-1 exerts these effects. Drawing upon previous studies demonstrating the modulation of inflammatory pathways by MR-1, we hypothesized that MR-1 could

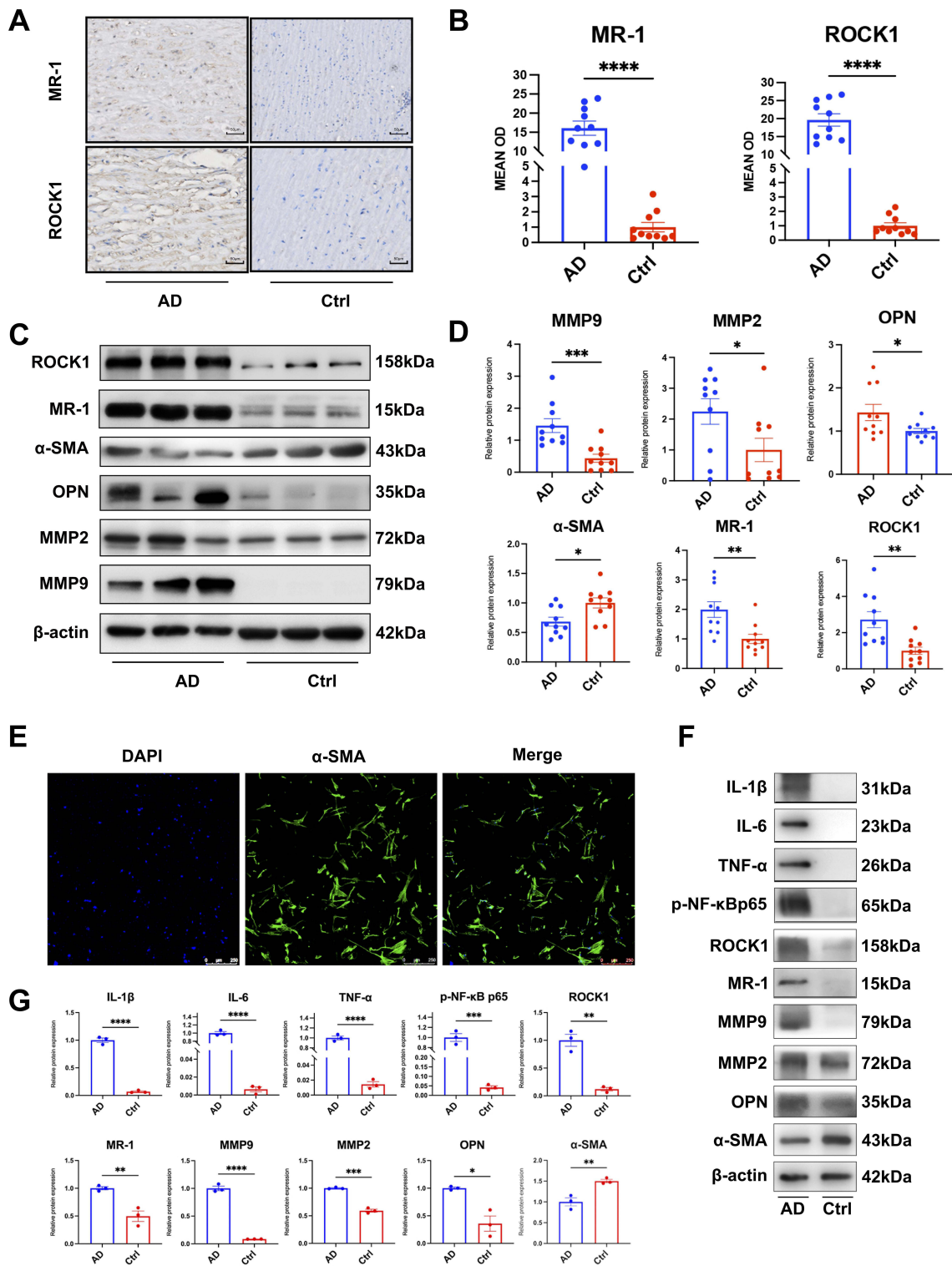


Figure 2 The expression levels of MR-1 and ROCK1 were found to be markedly upregulated in the aortas of the AD group. **(A)** Immunohistochemistry and **(B)** quantification of MR-1 (brown), ROCK1 (brown) in human aortas from AD and Ctrl groups (unpaired two-tailed Student's *t*-test with Welch's correction for MR-1, ROCK1). Each datapoint represents an individual human. *n*=10 human aortas (AD or Ctrl). **(C)** Western blot analysis and **(D)** quantification of ROCK, MR-1, α-SMA, OPN, MMP2 and MMP9 in human aortas with AD or Ctrl (unpaired two-tailed Student's *t*-test with Welch's correction for MR-1, ROCK). β-actin was used as a loading control. Data are shown as mean ± SEM. Each datapoint represents an individual human. *n*=10 human aortas (AD or Ctrl). All data are based on biological replicates. **(E)** Immunofluorescence was used to identify the purity of smooth muscle cells. Scale bar = 250 μm. **(F)** Western blot analysis and **(G)** quantification of MR-1, ROCK1 protein expression levels and inflammatory pathway activation levels in AD or Ctrl vSMCs (one-way ANOVA followed by Bonferroni post hoc test). *n*=3. Data are shown as mean±SEM. All data are based on biological replicates. The duplication occurred in **Figures 1D and 2C E** (β-actin) because the experimental conditions and sample sources for these groups were consistent. **P* < 0.05, ***P* < 0.01, ****P* < 0.001, *****P* < 0.0001.

further impact AD formation via its influence on the release of inflammatory factors. We analyzed the activation level of NF-kappaB p65, nuclear translocation, as well as the mRNA and protein expressions of inflammatory factors such as IL-1 β , IL-6, and TNF- α in the treatment group through protein immunoblotting, cellular immunofluorescence staining, and PCR techniques. Our findings revealed a significant increase in the activation level of NF-kappaB p65, the nuclear translocation level of NF-kappaB p65, and the expression of IL-1 β , IL-6 and TNF- α in the AD group compared to the control group. In addition, all indicators of the inflammatory pathway witnessed significant reductions subsequent to silencing MR-1 (See Figure 3C–F). Collectively, our results indicate that the overexpression of MR-1 in AD human aortic smooth muscle cells can activate NF-kappaB p65 through

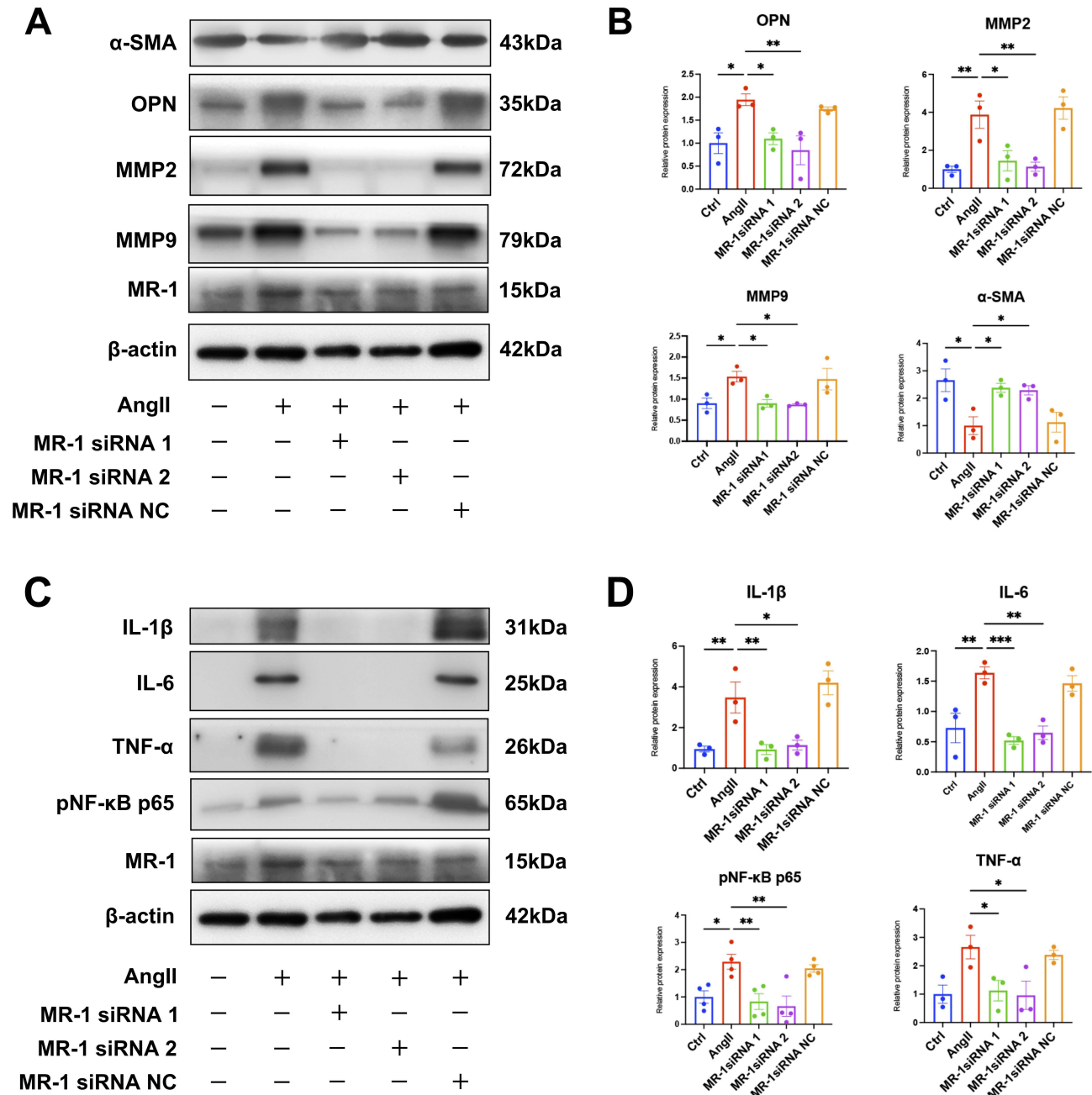


Figure 3 Continued.

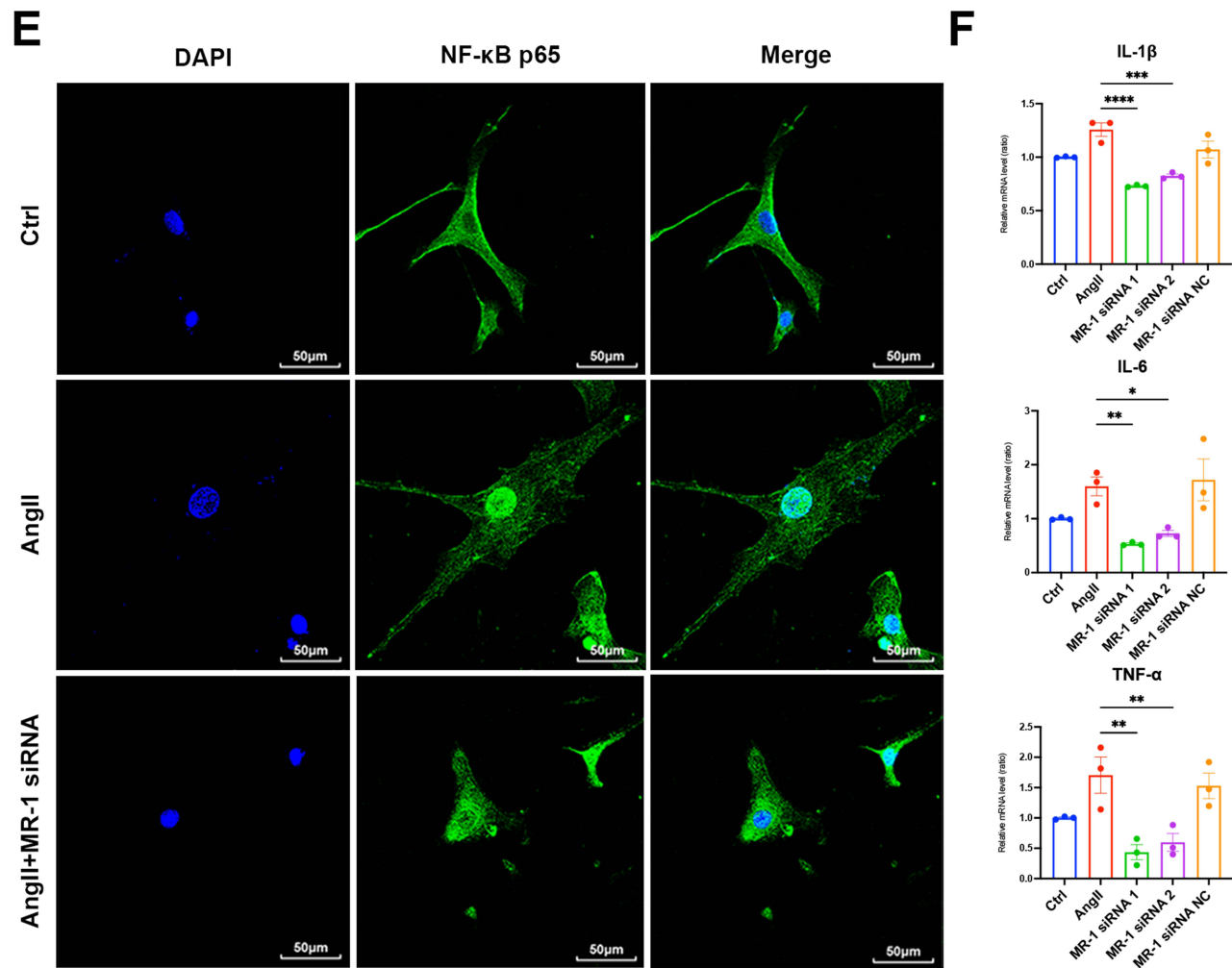


Figure 3 Inhibition of MR-1 reduces vSMCs inflammatory expression, inhibits vSMCs phenotypic transformation and ECM degradation. **(A)** Western blotting and quantification **(B)** of α -SMA, OPN, MMP2, MMP9 and MR-1 in the presence or absence of MR-1 siRNA in human vSMCs cultured in angiotensin II ($1\mu\text{M}$) for 24 h (one-way ANOVA followed by Bonferroni post hoc test). β -actin was used as a loading control. $n=3$. **(C)** AD smooth muscle cell model with or without MR-1 siRNA and Western blotting and quantification **(D)** of NF-kappaB p65 phosphorylation activation and levels of inflammatory factors IL-1 β , IL-6, and TNF- α release in the MR-1 siRNA NC group (one-way ANOVA followed by Bonferroni post hoc test). β -actin was used as a loading control. $n=3$. **(E)** Representative images of cellular immunofluorescence detection of NF-kappaB p65 (green) in angiotensin II-treated ($1\mu\text{M}$) human vSMCs in the presence or absence of MR-1 siRNA. Scale bar = $50\mu\text{m}$. **(F)** The mRNA levels of inflammatory factors IL-1 β , IL-6, and TNF- α release in the presence or absence of MR-1 siRNA in human vSMCs (one-way ANOVA followed by Bonferroni post hoc test). $n=3$. Data are shown as mean \pm SEM. All data are based on biological replicates. The duplication occurred in **Figures 3A** and **3C** (MR-1 and β -actin) because the experimental conditions and sample sources for these groups were consistent. * $P < 0.05$, ** $P < 0.01$, *** $P < 0.001$, **** $P < 0.0001$.

phosphorylation and facilitates its translocation into the nucleus, leading to the release of inflammatory factors IL-1 β , IL-6, and TNF- α . Furthermore, these findings suggest that MR-1 may regulate smooth muscle cell phenotypic transformation and extracellular matrix degradation, ultimately affecting the progression of AD. Such insights provide new perspectives on the potential mechanisms through which MR-1 may contribute to the pathogenesis of AD.

ROCK1 Affects Smooth Muscle Cell Phenotypic Transformation and Matrix Metalloproteinase Release by Regulating Inflammatory Factor Release

To further elucidate the specific mechanisms underlying the involvement of ROCK1 in AD formation, we conducted a comprehensive investigation employing a similar approach as the one utilized for studying the role of MR-1. Initially, we divided the experimental group into distinct categories, including normal human aortic smooth muscle cells (Ctrl group), dissected human aortic smooth muscle cells (AD group), dissected human aortic smooth muscle cells treated with ROCK1 siRNA 1/2 (ROCK1 siRNA 1/2 group), and ROCK1 siRNA Negative Control (ROCK1 siRNA NC group). By implementing

protein immunoblotting analyses, we observed a significant elevation in ROCK1 expression in the AD and ROCK1 siRNA NC groups compared to the Ctrl and ROCK1 siRNA 1/2 groups. Correspondingly, the expression levels of smooth muscle cell phenotypic transformation markers (α -SMA, OPN) and MMP9 altered alongside variations in ROCK1 expression. Relative to the AD group, the ROCK1 siRNA 1/2 group demonstrated increased expression of α -SMA and decreased expression of OPN and MMP9 (See Figure 4A and B). These observations underscore the potentiality of ROCK1 in influencing smooth muscle cell phenotypic transformation and extracellular matrix degradation, thereby potentially impacting the progression of AD. In the context of understanding its mode of action, we ventured to explore the interaction between ROCK1 and inflammatory pathways, premised on prior studies. Our investigation has unveiled that ROCK1 plays a pivotal role in modulating the

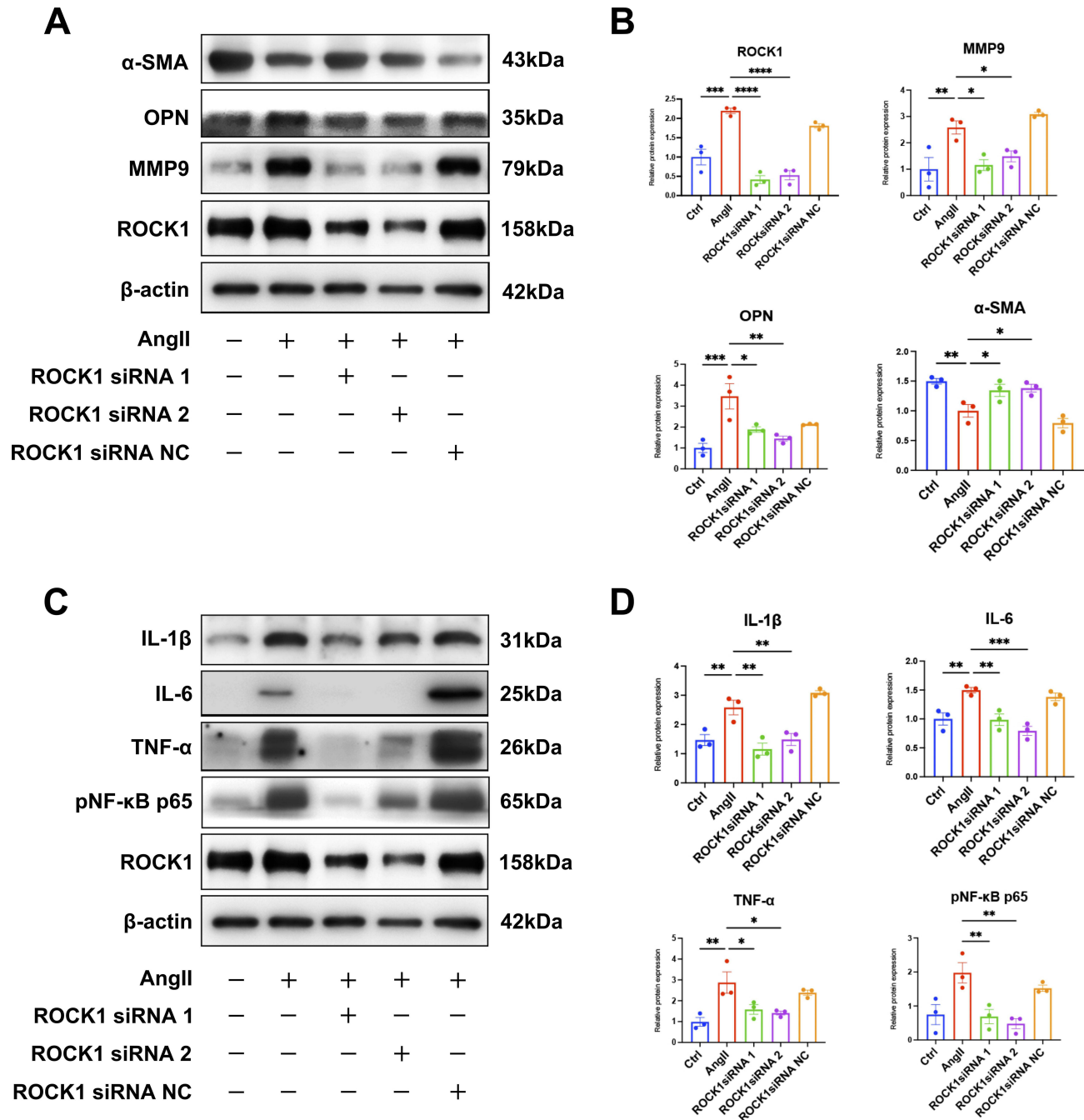


Figure 4 Continued.

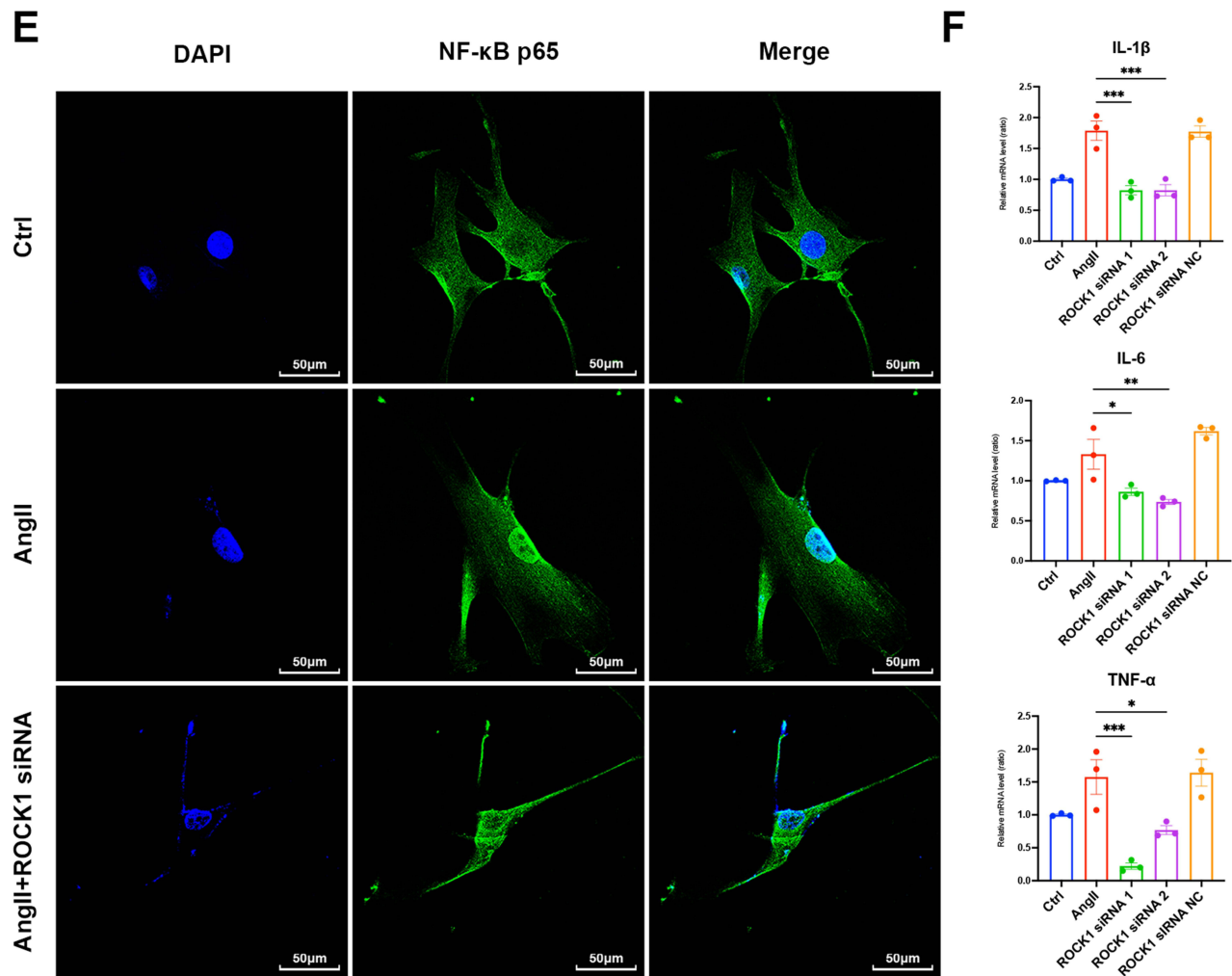


Figure 4 Inhibition of ROCK1 reduces vSMCs inflammatory expression, inhibits vSMCs phenotypic transformation and ECM degradation. **(A)** Western blotting and quantification **(B)** of α -SMA, OPN, MMP9 and ROCK1 in the presence or absence of ROCK1 siRNA in human vSMCs cultured in angiotensin II ($1\mu\text{M}$) for 24 h (one-way ANOVA followed by Bonferroni post hoc test). β -actin was used as a loading control. $n=3$. **(C)** AD smooth muscle cell model with or without ROCK1 siRNA and Western blotting and quantification **(D)** of NF-kappaB p65 phosphorylation activation and levels of inflammatory factors IL-1 β , IL-6, and TNF- α release in the ROCK1 siRNA NC group (one-way ANOVA followed by Bonferroni post hoc test). β -actin was used as a loading control. $n=3$. **(E)** Representative images of cellular immunofluorescence detection of NF-kappaB p65 (green) in angiotensin II-treated ($1\mu\text{M}$) human vSMCs in the presence or absence of ROCK1 siRNA. Scale bar = $50\mu\text{m}$. **(F)** The mRNA levels of inflammatory factors IL-1 β , IL-6, and TNF- α release in the presence or absence of ROCK1 siRNA in human vSMCs (one-way ANOVA followed by Bonferroni post hoc test). $n=3$. Data are shown as mean \pm SEM. All data are based on biological replicates. The duplication occurred in **Figures 4A** and **4C** (ROCK1 and β -actin) because the experimental conditions and sample sources for these groups were consistent. * $P < 0.05$, ** $P < 0.01$, *** $P < 0.001$, **** $P < 0.0001$.

activation level of NF-kappaB p65, the nuclear translocation level of NF-kappaB p65, along with influencing the mRNA and protein expression levels of key inflammatory factors, including IL-1 β , IL-6, and TNF- α (See **Figure 4C–F**). These findings collectively unravel the potential role of ROCK1 in modulating the progression of AD by regulating the expression levels of inflammatory pathways. The pivotal role of ROCK1 in impacting inflammatory cascades not only stands as a pertinent revelation in AD pathogenesis but also suggests the nuanced cross-talk between diverse signaling pathways and cellular processes, thereby shedding light on potential therapeutic avenues for mitigating AD progression. Expanding further upon these findings may provide a compelling framework for potential therapeutic interventions aimed at mitigating the progression of AD. Furthermore, by delving into the mechanistic underpinnings of ROCK1, this study facilitates a more comprehensive understanding of AD pathogenesis, potentially laying the groundwork for targeted therapies.

MR-1 Affects AD Progression by Regulating the ROCK1-NF-kappaB p65 Signaling Pathway

The aforementioned experiments underscore the pivotal roles played by MR-1 and ROCK1 in the modulation of smooth muscle cell phenotype transformation and ECM degradation. The regulation of NF-kappaB p65 activation and the release of various inflammatory factors—IL-1 β , IL-6, and TNF- α —are identified as critical avenues through which MR-1 and ROCK1 potentially impact the progression of aortic dissection. Encapsulating this premise, our study delved into investigating the interplay between MR-1 and ROCK1 in the regulation of AD progression. Initially, we embarked on elucidating the interaction relationship between MR-1 and ROCK1 with respect to the regulation of AD progression. First, we pursued co-localization analysis of MR-1 and immunofluorescent ROCK1 within human aortic smooth muscle cells from the dissection group, revealing a potential interaction between MR-1 and ROCK1 within these cells (Figure 5A and B). Subsequently, we

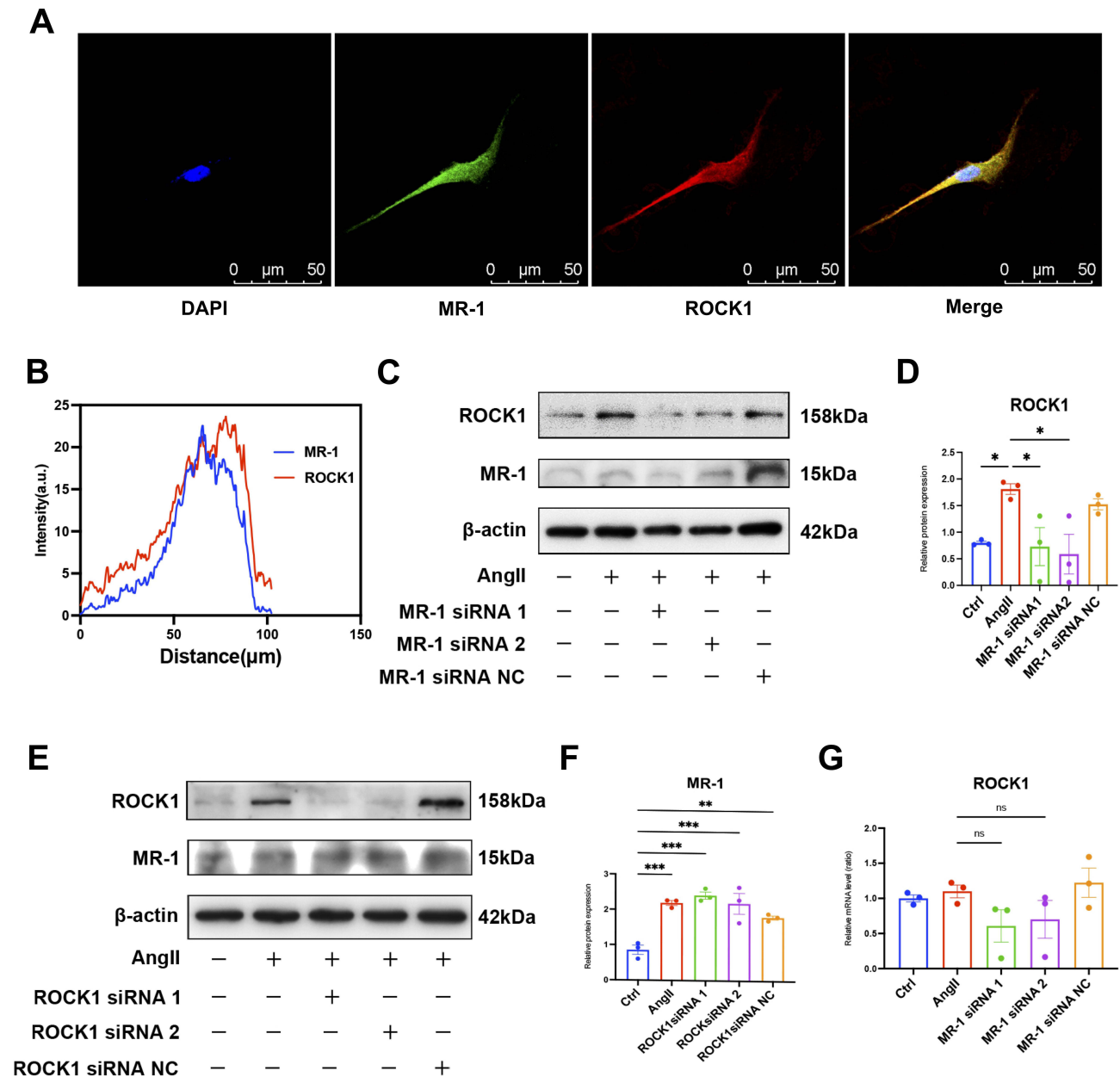


Figure 5 MR-1 Affects AD Progression by Regulating the ROCK1-NF-kappaB p65 Signaling Pathway. **(A and B)** Co-localization of MR-1 (green) with ROCK1 (red) in human vSMCs induced by angiotensinII for 24 hours. Scale bar= 50 μ m. **(C and D)** Protein immunoblotting and quantitative analysis of ROCK1 upon inhibition of MR-1 and **(E and F)** protein immunoblotting and quantitative analysis of MR-1 upon inhibition of ROCK1 in human vSMCs induced by angiotensinII for 24 hours (one-way ANOVA followed by Bonferroni post hoc test). β -actin was used as a loading control. n=3. **(G)** RT-PCR was performed to detect mRNA levels of ROCK1 in human vSMCs treated with angiotensinII in the presence or absence of MR-1 siRNA (one-way ANOVA followed by Bonferroni post hoc test). n=3. Data are shown as mean \pm SEM. All data are based on biological replicates. *P < 0.05, **P < 0.01, ***P < 0.001.

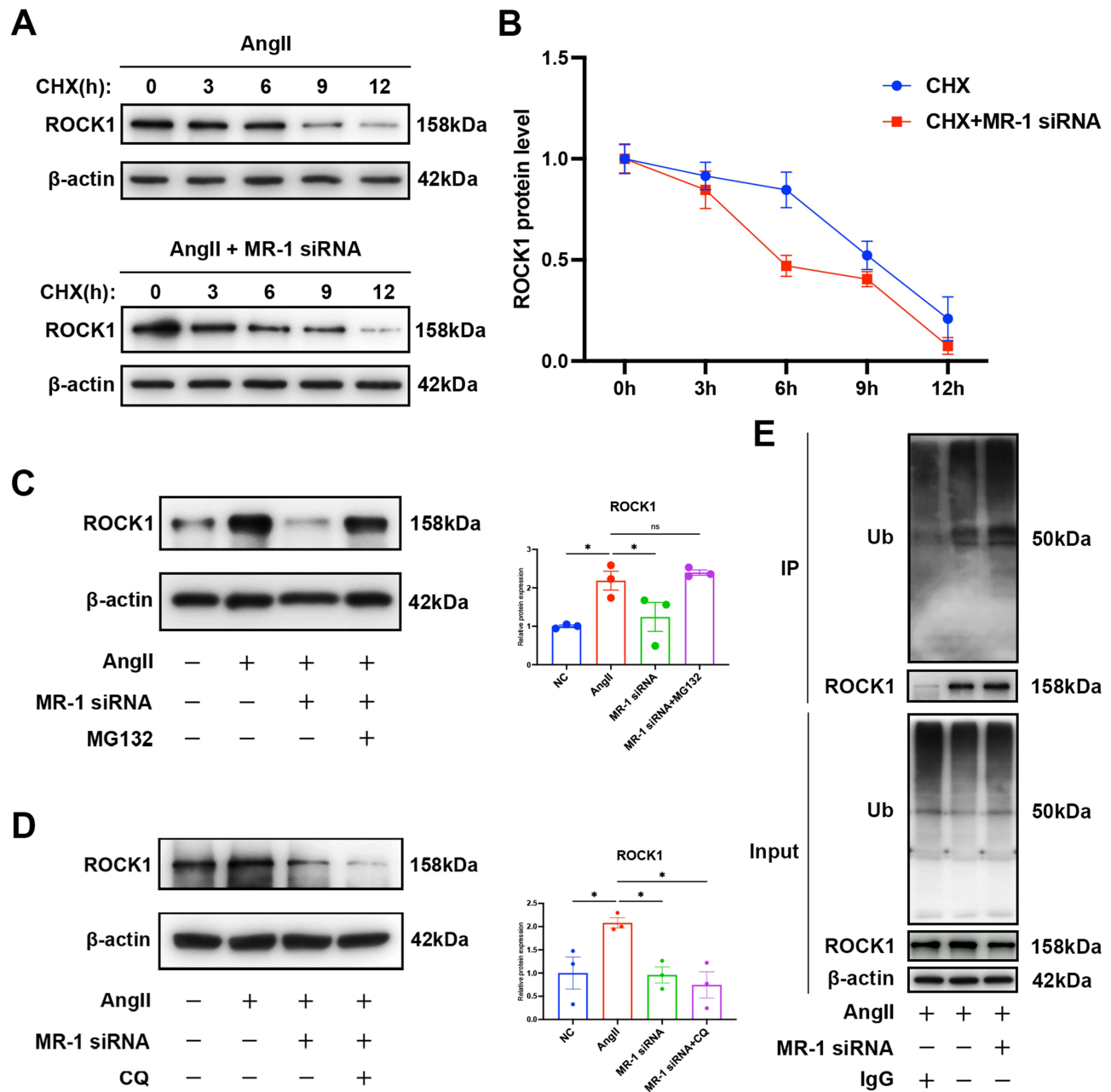


Figure 6 Increased expression of MR-1 inhibits ubiquitination and degradation of ROCK1. (A and B) Western blotting was performed to detect protein levels of ROCK1 in human vSMCs treated with cycloheximide (CHX, 10 μM) and angiotensin II for the indicated times in the presence or absence of MR-1 siRNA (one-way ANOVA followed by Bonferroni post hoc test). β-actin was used as a loading control. n=3. (C and D) After preincubation with MG132 (10 μM) or chloroquine (CQ, 10 μM) for 30 minutes, Western blotting was performed to detect the protein level of ROCK1 in angiotensin II -treated human vSMCs in the presence or absence of MR-1 siRNA (one-way ANOVA followed by Bonferroni post hoc test). β-actin was used as a loading control. n=3. (E) Co-IP was performed to detect the ubiquitination level of ROCK1 in angiotensin II -treated human vSMCs in the presence or absence of MR-1 siRNA. β-actin was used as a loading control. n=3. Data are shown as mean ± SEM. All data are based on biological replicates. *P < 0.05.

further delved into the intricate relationship through the evaluation of ROCK1 protein expression in MR-1 siRNA-treated groups and MR-1 protein expression in ROCK1 siRNA-treated groups, comparing these expressions with those of the AD group. Notably, we observed that the expression of ROCK1 in the MR-1 siRNA-treated group was altered in comparison to the AD group, while the MR-1 protein expression in the ROCK1 siRNA treated group did not show any changes related to the AD group (Figure 5C–F). These findings suggest that MR-1 has the capacity to positively regulate ROCK1 expression as

an upstream regulator. This aligns with our observation that in an angiotensin-stimulated dissected human aortic smooth muscle cell model, overexpression of MR-1 upregulates ROCK1 expression, thereby promoting the phosphorylation of NF-kappaB p65 and the release of inflammatory factors IL-1 β , IL-6, and TNF- α . Finally, to further probe into the specific mechanism underlying MR-1's regulation of ROCK1 expression, we examined the mRNA expression of ROCK1 in the group treated with MR-1 siRNA and made a comparison with that in the AD group (Figure 5G). It was discovered that the mRNA level of ROCK1 did not undergo significant changes after MR-1 expression was inhibited. This result implies that we should center on the post-translational modification of the protein when exploring the mechanism of ROCK1 regulation by MR-1.

MR-1 Stabilizes ROCK1 Protein by Suppressing Its Ubiquitination and Degradation

Previous experimental findings have indicated that the regulation of ROCK1 by MR-1 is likely to occur at the post-translational level of the protein. To explore whether MR-1 regulates ROCK1 by influencing its protein stability, we analyzed the protein expression level of ROCK1 in Human vSMCs treated with MR-1 siRNA, with the aid of the protein synthesis inhibitor cycloheximide (CHX). It was found that, compared to Human vSMCs without MR-1 siRNA treatment, the protein degradation rate of ROCK1 was accelerated once MR-1 expression was inhibited. Moreover, the suppression of MR-1 expression shortened the half-life of ROCK1 (Figure 6A and B). It is well-known that in eukaryotic cells, protein degradation mainly depends on two pathways - The ubiquitin - proteasome pathway and the autophagy - lysosome pathway. Subsequently, we treated the cells with MG132 (a proteasome inhibitor) and chloroquine (CQ, a lysosomal inhibitor) respectively. The results demonstrated that MG132 reversed the decrease in ROCK1 expression levels in Human vSMCs treated with MR-1 siRNA, while CQ did not have such an effect (Figure 6C and D). Co-IP analysis also revealed that, in contrast to the angiotensin II group, the inhibition of MR-1 expression led to an increased ubiquitination level of ROCK1 (Figure 6E). These results imply that MR-1 stabilizes ROCK1 by inhibiting its ubiquitin - proteasome degradation pathway. This concerted regulation instigates the transformation of smooth muscle cell phenotype from contractile to secretory type, along with ECM degradation, ultimately culminating in the development of AD. These insights not only unravel the intricate dynamics of the regulatory interplay between MR-1 and ROCK1 but also offer a comprehensive understanding of the molecular underpinnings governing AD progression. The prospective capacity of MR-1 and ROCK1 as potential regulators of inflammatory cascades and smooth muscle cell phenotype transformation presents a compelling avenue for developing targeted therapeutics in the context of AD.

Discussion

The pathogenesis of aortic dissection involves several critical aspects, with inflammation emerging as a pivotal factor. This has propelled anti-inflammatory therapy as a potential strategy for the treatment of aortic dissection.^{2,17,18} Notably, recent research has increasingly unveiled the roles of various inflammatory cells, such as macrophages, lymphocytes, and neutrophils, along with their secreted inflammatory factors in the formation of aortic dissection.^{5,19-26} While studies regarding the impact of MR-1 in the cardiovascular system have predominantly centered on promoting cardiac hypertrophy by MR-1 overexpression, its expression and function in large blood vessels and vascular smooth muscle remain largely unexplored.^{10,11,27} On the other hand, the role of ROCK1 in the cardiovascular system has garnered significant attention in recent years, where it regulates a myriad of cellular functions, including those in cardiomyocytes, endothelial cells, and smooth muscle cells, thereby exerting an effect on cardiac hypertrophy, angiogenesis, and other pathophysiological processes.^{12-14,28} Both MR-1 and ROCK1 modulate inflammatory pathways and regulate the degree of NF-KappaB p65 activation in the cardiovascular system. However, their specific roles in the aortic wall and the underlying mechanisms in aortic dissection remain less understood.^{10,11,15,29,30}

This study sought to demonstrate that MR-1 and ROCK1 promote the progression of aortic dissection by modulating inflammatory pathways. Specifically, we observed a significant upregulation of MR-1 and ROCK1 in human aortic dissection vessels, which facilitated the advancement of aortic dissection by activating inflammatory pathways.

In our exploration of the pathogenesis of aortic dissection, mounting evidence has highlighted the role of NF-KappaB p65 in promoting the progression of aortic dissection.^{20,22,23,31} Our analysis of blood indices in the AD group and control patients revealed an increase in inflammatory cells in the AD group, while examination of aortic tissues from AD and control patients confirmed the activation of NF-KappaB p65 by phosphorylation in human aorta afflicted with AD. This was accompanied by the release of sizable amounts of inflammatory factors such as TNF- α , IL-1 β , and IL-6. Furthermore, *in vitro* experiments utilizing an aortic smooth muscle cell model of AD validated these results.

The role of MR-1 in vascular and smooth muscle cells has remained relatively unexplored in previous studies. Yet, it has been observed that overexpression of MR-1 enhances angiotensin-induced NF-KappaB activation in cardiomyocytes, while down-regulation of MR-1 blocks NF-KappaB activation, indicating its potential influence on the development of cardiovascular system diseases through inflammation.¹⁰ We hypothesized that MR-1 is similarly expressed to some extent in smooth muscle cells, a conjecture that we verified in aortic tissues and cellular models. Specifically, we found that the expression of MR-1 was significantly higher in aortic tissues of AD patients compared to controls. In addition, the elevated expression of MR-1 in vSMCs induced by angiotensin II promoted the phosphorylation of NF-KappaB p65, the nuclear translocation of NF-kappaB p65, the release of multiple inflammatory factors as well as the release of MMPs. These mechanisms contributed to the transition of smooth muscle cell phenotype from contractile to secretory, ultimately driving the progression of AD. In conclusion, we identified that MR-1 is overexpressed in entrapped aorta and smooth muscle cells and affects AD progression by regulating inflammation.

Studies on the role of ROCK1 in cardiovascular system diseases have provided valuable insights, as ROCK1 is abundantly expressed in smooth muscle cells and can regulate their function through various mechanisms, including inflammation.^{13,14} For example, it has been demonstrated that ROCK1 regulates smooth muscle phenotypic modulation and vascular remodeling through the JNK pathway and the wave protein cytoskeleton.³² Meanwhile, the inhibition of ROCK1 expression has been linked to the attenuation of ROCK-1 phosphorylation of MRTF-A, thus inhibiting the expression of collagen and fibronectin proteins, exerting a protective effect during the conversion of vSMCs to myofibroblasts.¹⁵ Our study revealed that the level of ROCK1 protein expression in aortic tissues of the AD group was significantly higher compared to the control group. Additionally, *in vitro* experiments showed that overexpression of ROCK1 facilitated the phenotypic transformation of vSMCs and ECM degradation through the inflammatory pathway. Conversely, inhibition of ROCK1 reduced the activation level of the inflammatory pathway, the degree of vSMCs phenotypic transformation, and the level of ECM degradation. Taken together, our findings highlighted the influential role of ROCK1 in the progression of AD through the inflammatory pathway.

As a common protein modification within organisms, ubiquitination plays an indispensably crucial role in regulating protein stability. Ubiquitination is an enzyme-mediated cascade reaction that takes place through the enzymatic functions of E1 (ubiquitin (Ub)-activating enzyme), E2 (Ub-conjugating enzyme), and E3 (Ub-ligase), and this process can be repressed by deubiquitinating enzymes (DUB). Previous research has indicated that both MR-1 and ROCK1 participate in a variety of ubiquitin-mediated pathophysiological processes in organisms. During the progression of non-small-cell lung cancer (NSCLC), an elevation in the level of MR-1 impacts the phosphorylation level of ITCH and diminishes its E3 enzyme activity, thereby causing a reduction in the ubiquitination-mediated degradation of NICD3.³³ In the exploration of therapeutic targets for colorectal cancer, it has been discovered that TRIM40 can directly bind to and ubiquitinate the ROCK1 protein, accelerating its degradation. This, in turn, reduces the stability of the c-Myc protein and inhibits the proliferation of colorectal cancer cells.³⁴ These studies establish a solid theoretical basis for our further exploration of the interaction between MR-1 and ROCK1. In our study, we have found that the inhibition of MR-1 significantly decreases the expression level of the ROCK1 protein. Conversely, after the inhibition of ROCK1, the expression of MR-1 does not change significantly, and MR-1 has no impact on the ROCK1 expression at the mRNA level. This result implies that we should further investigate the regulatory mechanism of MR-1 on ROCK1 with a focus on the post-translational modification of proteins. Our study reveals that the up-regulation of MR-1 expression restrains the ubiquitination-associated binding and protein degradation of ROCK1, resulting in an increase in the protein level of ROCK1.

In terms of limitations, we merely simulated the aortic dissection model within human tissues and *in vitro* smooth muscle cells. Based on this simulation, we probed into the pathological process in which MR-1 and ROCK1 regulate the inflammatory pathway and thereby impact aortic dissection. Nevertheless, we were short of animal experiments capable of replicating the intricate biological processes *in vivo*. This is also the aspect that we intend to further explore in the future. In addition, our experimental protocol did not involve the application of MR-1 and ROCK1 inhibitors or other drugs to investigate the impacts on their interaction and the progression of aortic dissection. Considering the molecular mechanisms we have proposed, carrying out such experiments will offer more convincing evidence for the future clinical utilization of drugs targeting MR-1 and ROCK1 in the treatment of aortic dissection.

In conclusion, aortic dissection remains a significant cardiovascular emergency with inflammation being a key factor in its development. This study has comprehensively explored the roles of MR-1 and ROCK1 in aortic dissection. Through various

experiments, including analyses of aortic tissues and in vitro models, it was shown that MR-1 and ROCK1 are upregulated in aortic dissection patients and are associated with smooth muscle cell phenotypic changes and matrix metalloproteinase release via inflammatory pathways. The relationship between MR-1 and ROCK1 was also elucidated, with MR-1 acting as an upstream regulator of ROCK1. For future research, in addition to the previously mentioned animal experiments and drug inhibitor studies, it would be valuable to further investigate how ROCK1 regulates the aortic endothelial barrier function and its impact on aortic dissection progression. This could involve in-depth studies on the molecular mechanisms underlying ROCK1's influence on endothelial cell junctions, permeability, and interactions with other cells in the aortic wall. This would provide more evidence for the clinical utilization of drugs targeting MR-1 and ROCK1 in treating aortic dissection.

Data Sharing Statement

The raw data supporting the conclusions of this article will be made available by the authors, without undue reservation.

Ethical Approval

Human aortic tissues were obtained in accordance with the Declaration of Helsinki and under informed consent using protocols approved by the Ethics Committee of Qilu Hospital of Shandong University (approval number: KYLL-202208-005).

Acknowledgments

The authors thank all members of the Emergency Department of Qilu Hospital of Shandong University for their valuable comments on the manuscript.

Author Contributions

All authors made a significant contribution to the work reported, whether that is in the conception, study design, execution, acquisition of data, analysis and interpretation, or in all these areas; took part in drafting, revising or critically reviewing the article; gave final approval of the version to be published; have agreed on the journal to which the article has been submitted; and agree to be accountable for all aspects of the work.

Funding

We acknowledge funding from the National Natural Science Foundation of China (82170442, 82070388 and 82370378), Taishan Scholar Project of Shandong Province (tsqn202211310 and tspd20181220), Natural Science Foundation of Shandong Province (ZR2020MH035), National Key R&D Program of China (2020YFC1512700, 2020YFC1512705, 2020YFC1512703, 2022YFC0868600), National Science & Technology Fundamental Resources Investigation Project (2018FY100600, 2018FY100602), The Interdisciplinary Young Researcher Groups Program of Shandong University (2020QNQT004), Youth Top-Talent Project of National Ten Thousand Talents Plan and Qilu Young Scholar Program.

Disclosure

The authors report no conflicts of interest in this work.

References

1. Liu H, Zhang Y, Song W, Sun Y, Jiang Y. Osteopontin N-terminal function in an abdominal aortic aneurysm from apolipoprotein E-deficient mice. *Front Cell Dev Biol.* 2021;9:681790. doi:10.3389/fcell.2021.681790
2. Shen YH, LeMaire SA, Webb NR, Cassis LA, Daugherty A, Lu HS. Aortic aneurysms and dissections series. *Arterioscler Thromb Vasc Biol.* 2020;40(3):e37–e46. doi:10.1161/ATVBAHA.120.313991
3. Bossone E, Eagle KA. Epidemiology and management of aortic disease: aortic aneurysms and acute aortic syndromes. *Nat Rev Cardiol.* 2021;18(5):331–348. doi:10.1038/s41569-020-00472-6
4. Waldmuller S, Muller M, Warnecke H, et al. Genetic testing in patients with aortic aneurysms/dissections: a novel genotype/phenotype correlation? *Eur J Cardiothorac Surg.* 2007;31(6):970–975. doi:10.1016/j.ejcts.2007.02.027
5. He R, Guo DC, Estrera AL, et al. Characterization of the inflammatory and apoptotic cells in the aortas of patients with ascending thoracic aortic aneurysms and dissections. *J Thorac Cardiovasc Surg.* 2006;131(3):671–678. doi:10.1016/j.jtcvs.2005.09.018
6. Lopez-Candales A, Holmes DR, Liao S, Scott MJ, Wickline SA, Thompson RW. Decreased vascular smooth muscle cell density in medial degeneration of human abdominal aortic aneurysms. *Am J Pathol.* 1997;150(3):993–1007.

7. Galis ZS, Sukhova GK, Lark MW, Libby P. Increased expression of matrix metalloproteinases and matrix degrading activity in vulnerable regions of human atherosclerotic plaques. *J Clin Invest.* 1994;94(6):2493–2503. doi:10.1172/JCI117619
8. Wang X, Zhang X, Qiu T, Yang Y, Li Q, Zhang X. Dexamethasone reduces the formation of thoracic aortic aneurysm and dissection in a murine model. *Exp Cell Res.* 2021;405(2):112703. doi:10.1016/j.yexcr.2021.112703
9. Li TB, Liu XH, Feng S, et al. Characterization of MR-1, a novel myofibrillogenesis regulator in human muscle. *Acta Biochim Biophys Sin (Shanghai).* 2004;36(6):412–418. doi:10.1093/abbs/36.6.412
10. Li HL, She ZG, Li TB, et al. Overexpression of myofibrillogenesis regulator-1 aggravates cardiac hypertrophy induced by angiotensin II in mice. *Hypertension.* 2007;49(6):1399–1408. doi:10.1161/HYPERTENSIONAHA.106.085399
11. Wang Q, Wang Y, Zhang J, Pan S, Liu S. Silencing MR-1 protects against myocardial injury induced by chronic intermittent hypoxia by targeting Nrf2 through antioxidant stress and anti-inflammation pathways. *J Healthc Eng.* 2022;2022:3471447. doi:10.1155/2022/3471447
12. Ellawindy A, Satoh K, Sunamura S, et al. Rho-kinase inhibition during early cardiac development causes arrhythmogenic right ventricular cardiomyopathy in mice. *Arterioscler Thromb Vasc Biol.* 2015;35(10):2172–2184. doi:10.1161/ATVBAHA.115.305872
13. Kimura K, Ito M, Amano M, et al. Regulation of myosin phosphatase by Rho and Rho-associated kinase (Rho-kinase). *Science.* 1996;273(5272):245–248. doi:10.1126/science.273.5272.245
14. Chen M, Zhang Y, Li W, Yang J. MicroRNA-145 alleviates high glucose-induced proliferation and migration of vascular smooth muscle cells through targeting ROCK1. *Biomed Pharmacother.* 2018;99:81–86. doi:10.1016/j.biopha.2018.01.014
15. Zou F, Li Y, Zhang S, Zhang J. DP1 (Prostaglandin D(2) Receptor 1) activation protects against vascular remodeling and vascular smooth muscle cell transition to myofibroblasts in angiotensin ii-induced hypertension in mice. *Hypertension.* 2022;79(6):1203–1215. doi:10.1161/HYPERTENSIONAHA.121.17584
16. Wang Y, Zheng XR, Riddick N, et al. ROCK isoform regulation of myosin phosphatase and contractility in vascular smooth muscle cells. *Circ Res.* 2009;104(4):531–540. doi:10.1161/CIRCRESAHA.108.188524
17. Al-Rifai R, Vandestienne M, Lavillegrand JR, et al. JAK2V617F mutation drives vascular resident macrophages toward a pathogenic phenotype and promotes dissecting aortic aneurysm. *Nat Commun.* 2022;13(1):6592. doi:10.1038/s41467-022-34469-1
18. Sudhakar V, Das A, Horimatsu T, et al. Copper Transporter ATP7A (Copper-Transporting P-Type ATPase/Menkes ATPase) limits vascular inflammation and aortic aneurysm development: role of MicroRNA-125b. *Arterioscler Thromb Vasc Biol.* 2019;39(11):2320–2337. doi:10.1161/ATVBAHA.119.313374
19. Del Porto F, Proietta M, Tritapepe L, et al. Inflammation and immune response in acute aortic dissection. *Ann Med.* 2010;42(8):622–629. doi:10.3109/07853890.2010.518156
20. Ju X, Ijaz T, Sun H, et al. Interleukin-6-signal transducer and activator of transcription-3 signaling mediates aortic dissections induced by angiotensin II via the T-helper lymphocyte 17-interleukin 17 axis in C57BL/6 mice. *Arterioscler Thromb Vasc Biol.* 2013;33(7):1612–1621. doi:10.1161/ATVBAHA.112.301049
21. Anzai A, Shimoda M, Endo J, et al. Adventitial CXCL1/G-CSF expression in response to acute aortic dissection triggers local neutrophil recruitment and activation leading to aortic rupture. *Circ Res.* 2015;116(4):612–623. doi:10.1161/CIRCRESAHA.116.304918
22. Tieu BC, Lee C, Sun H, et al. An adventitial IL-6/MCP1 amplification loop accelerates macrophage-mediated vascular inflammation leading to aortic dissection in mice. *J Clin Invest.* 2009;119(12):3637–3651. doi:10.1172/JCI38308
23. Zhang L, Liao MF, Tian L, et al. Overexpression of interleukin-1beta and interferon-gamma in type I thoracic aortic dissections and ascending thoracic aortic aneurysms: possible correlation with matrix metalloproteinase-9 expression and apoptosis of aortic media cells. *Eur J Cardiothorac Surg.* 2011;40(1):17–22. doi:10.1016/j.ejcts.2010.09.019
24. Yuan SM, Wang J, Huang HR, Jing H. Osteopontin expression and its possible functions in the aortic disorders and coronary artery disease. *Rev Bras Cir Cardiovasc.* 2011;26(2):173–182. doi:10.1590/s0102-76382011000200006
25. Longo GM, Xiong W, Greiner TC, Zhao Y, Fiotti N, Baxter BT. Matrix metalloproteinases 2 and 9 work in concert to produce aortic aneurysms. *J Clin Invest.* 2002;110(5):625–632. doi:10.1172/JCI15334
26. Moehle CW, Bhamidipati CM, Alexander MR, et al. Bone marrow-derived MCP1 required for experimental aortic aneurysm formation and smooth muscle phenotypic modulation. *J Thorac Cardiovasc Surg.* 2011;142(6):1567–1574. doi:10.1016/j.jtcvs.2011.07.053
27. Frey N, Katus HA, Olson EN, Hill JA. Hypertrophy of the heart: a new therapeutic target? *Circulation.* 2004;109(13):1580–1589. doi:10.1161/01.CIR.0000120390.68287.BB
28. Pillay LM, Yano JJ, Davis AE, et al. In vivo dissection of RhoA function in vascular development using zebrafish. *Angiogenesis.* 2022;25(3):411–434. doi:10.1007/s10456-022-09834-9
29. Tu PC, Pan YL, Liang ZQ, et al. Mechanical Stretch Promotes Macrophage Polarization and Inflammation via the RhoA-ROCK/NF-κB Pathway. *Biomed Res Int.* 2022;2022(1):6871269. doi:10.1155/2022/6871269
30. Shimokawa H, Sunamura S, Satoh K. RhoA/Rho-Kinase in the Cardiovascular System. *Circ Res.* 2016;118(2):352–366. doi:10.1161/CIRCRESAHA.115.306532
31. Wang X, Li Q, Li W, et al. Dexamethasone attenuated thoracic aortic aneurysm and dissection in vascular smooth muscle cell Tgfb2-disrupted mice with CCL8 suppression. *Exp Physiol.* 2022;107(6):631–645. doi:10.1113/EP090190
32. Tang L, Dai F, Liu Y, et al. RhoA/ROCK signaling regulates smooth muscle phenotypic modulation and vascular remodeling via the JNK pathway and vimentin cytoskeleton. *Pharmacol Res.* 2018;133:201–212. doi:10.1016/j.phrs.2018.05.011
33. Zhao W, Li Y, Cheng H, et al. Myofibrillogenesis regulator-1 regulates the ubiquitin lysosomal pathway of notch3 intracellular domain through E3 ubiquitin-protein ligase itchy homolog in the metastasis of non-small cell lung cancer. *Adv Sci (Weinh).* 2024;11(15):e2306472. doi:10.1002/advs.202306472
34. Hu F, Zhao L, Wang J, et al. TRIM40 interacts with ROCK1 directly and inhibits colorectal cancer cell proliferation through the c-Myc/p21 axis. *Biochim Biophys Acta Mol Cell Res.* 2024;1871(8):119855. doi:10.1016/j.bbamer.2024.119855

Journal of Inflammation Research

Dovepress

Taylor & Francis Group

Publish your work in this journal

The Journal of Inflammation Research is an international, peer-reviewed open-access journal that welcomes laboratory and clinical findings on the molecular basis, cell biology and pharmacology of inflammation including original research, reviews, symposium reports, hypothesis formation and commentaries on: acute/chronic inflammation; mediators of inflammation; cellular processes; molecular mechanisms; pharmacology and novel anti-inflammatory drugs; clinical conditions involving inflammation. The manuscript management system is completely online and includes a very quick and fair peer-review system. Visit <http://www.dovepress.com/testimonials.php> to read real quotes from published authors.

Submit your manuscript here: <https://www.dovepress.com/journal-of-inflammation-research-journal>